Fermi National Accelerator Laboratory

FERMILAB-FN-578

Higher-Order Momentum Compaction for a Simplified FODO Lattice and Comparison with SYNCH

K-Y. Ng

Fermi National Accelerator Laboratory
P.O. Box 500, Batavia, Illinois 60510

December 1991

Operated by Universities Research Association Inc. under Contract No. DE-AC02-76CHO3000 with the United States Department of Energy

Disclaimer

Distribution

ERRATA

for

HIGHER-ORDER MOMENTUM COMPACTION FOR A SIMPLIFIED FODO LATTICE AND COMPARISON WITH SYNCH

King-Yuen Ng

Fermi National Accelerator Laboratory, P.O. Box 500, Batavia, IL 60510*

(October, 1997)

The article, *Higher-order Momentum Compaction for a Simplified FODO Lattice and Comparison with Synch*, published as Fermilab-FN-578 in December of 1991, contains the following known typos:

1. In Eq. (3.11) on page 7, the second "sin" on the second line should be "cos"; or the correct equation should read

$$\left[x\cos\frac{\theta_0}{2}+y\sin\frac{\theta_0}{2}+\rho\sin\frac{S\hat{\eta}\delta}{1+\delta}\right]^2+$$
$$\left[-x\sin\frac{\theta_0}{2}+y\cos\frac{\theta_0}{2}-\rho_0-\hat{\eta}\delta+\rho\cos\frac{S\hat{\eta}\delta}{1+\delta}\right]^2=\rho^2\ . \qquad (3.10)$$

*Operated by the Universities Research Association, Inc., under contract with the U.S. Department of Energy.

2. In Eq. (3.12) on page 7, the second "sin" on the second line should be "cos"; or the correct equation should read

$$\left[x\cos\frac{\theta_0}{2} - y\sin\frac{\theta_0}{2} + \rho\sin\frac{S\check{\eta}\delta}{1+\delta}\right]^2 + \left[x\sin\frac{\theta_0}{2} + y\cos\frac{\theta_0}{2} - \rho_0 - \check{\eta}\delta + \rho\cos\frac{S\check{\eta}\delta}{1+\delta}\right]^2 = \rho^2 \ . \tag{3.11}$$

3. In Eq (3.13) on page 7, $-\rho_0$ has been left out in two occasions; or the correct equation should read

$$\rho\sin\frac{S\hat{\eta}\delta}{1+\delta} - \left[\rho\cos\frac{S\hat{\eta}\delta}{1+\delta} - \hat{\eta}\delta - \rho_0\right]t = \rho\sin\frac{S\check{\eta}\delta}{1+\delta} + \left[\rho\cos\frac{S\check{\eta}\delta}{1+\delta} - \hat{\eta}\delta - \rho_0\right]t \ , \tag{3.12}$$

4. In Eq. (3.24) on page 9, θ_0 should be θ_0^2; or the correct equation should read

$$\alpha_0 \to \frac{\theta_0^2(1 - S^2/12)}{S^2} \ . \tag{3.23}$$

5. Table II shown on page 13 is essentially the situation for 150 FODO cells. The correct Table II for 15 FODO cells is shown below:

Note: For a discussion of the next higher order momentum-compaction factor α_2, please refer to Fermilab Internal Report Conf-96/370: K.Y. Ng, *Reliability of α_1 and α_2 from Lattice Codes*, published in *New Directions for High-Energy Physics*, Snowmass 96, APS, p.233. The notations are slightly different in that article. The dispersion function has been denoted by D instead. The higher-order momentum compaction factors α_i, $i \geq 1$ there correspond to $\alpha_0\alpha_i$ here. Also, in the second paragraph of Section IIC, "half sextupole strength" should read "half quadrupole strength."

S	γ_{t0}	α_1		
		SYNCH	Theory	Difference
0.001	1.00001	0.000	0.000	0.000
0.010	1.00114	−0.001	0.000	−0.001
0.020	1.00457	0.000	0.000	0.000
0.040	1.01814	0.001	0.002	0.000
0.060	1.04038	0.009	0.009	0.000
0.080	1.07076	0.024	0.024	0.000
0.080	1.10860	0.051	0.026	0.025
0.120	1.15321	0.092	0.092	0.000
0.140	1.20383	0.144	0.144	0.000
0.160	1.25977	0.204	0.205	−0.001
0.180	1.32036	0.272	0.273	−0.002
0.200	1.38503	0.345	0.345	0.000
0.250	1.56128	0.523	0.525	−0.002
0.300	1.75354	0.689	0.691	−0.002
0.350	1.95754	0.831	0.833	−0.002
0.400	2.17040	0.950	0.953	−0.003
0.450	2.39025	1.049	1.052	−0.003
0.500	2.61582	1.133	1.136	−0.003
0.550	2.84628	1.200	1.208	−0.008
0.600	3.08108	1.268	1.271	−0.003
0.650	3.31988	1.321	1.326	−0.005
0.700	3.56247	1.371	1.377	−0.006
0.750	3.80873	1.417	1.424	−0.007
0.800	4.05865	1.465	1.468	−0.003
0.850	4.31226	1.512	1.511	0.002
0.900	4.56963	1.559	1.552	0.007
0.950	4.83088	1.592	1.593	−0.002
0.970	4.93651	1.610	1.610	0.000
0.980	4.98957	1.615	1.618	−0.003

FN-578

HIGHER-ORDER MOMENTUM COMPACTION FOR A SIMPLIFIED FODO LATTICE AND COMPARISON WITH SYNCH

King-Yuen Ng

Fermi National Accelerator Laboratory, P.O. Box 500, Batavia, IL 60510*

(December, 1991)

*Operated by the Universities Research Association, Inc., under contract with the U.S. Department of Energy.

I. INTRODUCTION

In a circular accelerator, particles with different momenta p have different closed-orbit lengths C which can be expanded around the momentum p_0 of the synchronous particle in the form[1]

$$C(p) = C_0[1 + \alpha_0\delta(1 + \alpha_1\delta) + \cdots] , \tag{1.1}$$

where C_0 is the orbit length of the synchronous particle and

$$\delta = \frac{p - p_0}{p_0} . \tag{1.2}$$

The linear coefficient α_0 is called the momentum compaction, which determines the momentum of the synchronous particle when it crosses transition. The first nonlinear coefficient α_1 determines when the off-momentum particles cross transition. For example, when $\alpha_1 \approx -3/2$, all the off-momentum particles cross transition at the same time as the synchronous particle.[1] As a result, there will not be any distortion of the bunch in the longitudinal phase space. Beam loss can therefore be minimized if the momentum aperture is large enough and the effects due to space charge and other coupling impedances are under controlled. There has also been suggestion of storage rings running near transition, the so-called isochronous rings.[2] There, most of the momentum compaction contribution comes from the nonlinear term. Thus, the knowledge of the value of α_1 and its possible modification are extremely valuable for the performance of an accelerator.

The calculation of α_1 for a simplified lattice consisting of only FODO cells of thin quadrupoles and dipoles filling all spaces had been reported.[3] However, when a check was made using the lattice code[4] SYNCH, it was found that the SYNCH results were different[5] from the values given by the derived analytic expression. The discrepancy even led some of us to believe that SYNCH might be wrong.

Recently, careful review of the analytic derivation and detailed study of some CERN papers[6] revealed that the derivation in Ref. 3 was not complete because a wiggling term had not been included. This is a consequence of the fact that the off-momentum orbit is not always "parallel" to the designed orbit. In this paper, we derive the exact analytic formula for α_1 in this simple FODO lattice and show that it agrees with the SYNCH results perfectly.

II. THE WIGGLING TERM

In Fig. 1, a particle with momentum p at B travels an infinitesimal vector of length $d\ell$ while the synchronous particle at A moves through an angle $d\theta_0$ or a length ds along the designed orbit. The transverse displacement x is denoted by AB. The length element $d\ell_0$ drawn "parallel" to or concentric with ds is given by

$$d\ell_0 = ds\left(1 + \frac{x}{\rho_0}\right) \tag{2.1}$$

where $\rho_0 = ds/d\theta_0$ is the radius of curvature of the designed orbit at A. Note that $d\ell$ and $d\ell_0$ are not the same, but are related by

$$d\ell_0 = d\ell \cos x' + \mathcal{O}(\delta^3)\ , \tag{2.2}$$

where $x' = dx/ds$. The fractional difference in total closed-orbit length is obtained by the integration

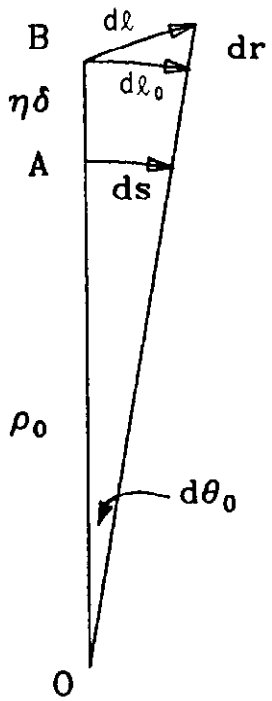

Figure 1: Derivation of the wiggling term and the differential equation for the momentum dispersion function.

$$\frac{\Delta C}{C_0} = \frac{1}{C_0}\int_C [d\ell - ds] \ . \tag{2.3}$$

Or with the aid of Eqs. (2.1) and (2.2),

$$\frac{\Delta C}{C_0} = \frac{1}{C_0}\int_C \left[\frac{1}{\cos x'}\left(1+\frac{x}{\rho_0}\right) - 1\right]\rho_0 d\theta \ . \tag{2.4}$$

By introducing the momentum dispersion function

$$\eta = \frac{x}{\delta} \ , \tag{2.5}$$

and expanding the cosine to second order in δ, we obtain

$$\frac{\Delta C}{C_0} = \frac{1}{C_0}\int_C ds\left(\frac{\eta\delta}{\rho_0} + \frac{\eta'^2\delta^2}{2} + \mathcal{O}(\delta^3)\right) \ . \tag{2.6}$$

If we further expand the momentum dispersion function around p_0 according to

$$\eta = \eta_0 + \eta_1\delta + \mathcal{O}(\delta^2) \ , \tag{2.7}$$

and compare the result with Eq. (1.1), we obtain finally

$$\alpha_0 = \frac{1}{C_0}\int_C ds\frac{\eta_0}{\rho_0} \ , \tag{2.8}$$

$$\alpha_0\alpha_1 = \frac{1}{C_0}\int_C ds\left(\frac{\eta_1}{\rho_0} + \frac{\eta'^2}{2}\right) \ . \tag{2.9}$$

The second term in Eq. (2.9) is called the wiggling term, whose presence is a result of the fact that the off-momentum orbit is not necessary "parallel" to or concentric with the designed orbit. Note that this derivation is also valid in the non-bending part of the ring where the radius of curvature $\rho_0 = \infty$. In that case the length elements $d\ell_0$ and ds are equal and only the wiggling term contributes. The wiggling term has been neglected in Ref. 2 in the computation of α_1, which constitutes the main disagreement of the results from SYNCH.

For a FODO cell, the dispersions at the F- and D-quadrupoles are respectively

$$\hat{\eta}_0 \approx \frac{\ell_0\theta_0(1+S/2)}{S^2} \ , \qquad \check{\eta}_0 \approx \frac{\ell_0\theta_0(1-S/2)}{S^2} \ , \tag{2.10}$$

to lowest order in θ_0, the bending angle of a half-cell dipole. In the above, ℓ_0 is the half-cell length and

$$S = \ell_0 \left| \int ds \frac{B'}{B_0 \rho_0} \right| , \tag{2.11}$$

where the last integral is the integrated strength of a half-quadrupole. Note that S is also equal to the sine of the half-cell phase advance if the centrifugal focussing is neglected. Thus, we have roughly

$$\alpha_0 \sim \frac{\theta_0^2}{S^2} \quad \text{and} \quad \frac{1}{C_0} \int_C ds \frac{\eta'^2}{2} \sim \frac{\theta_0^2}{2S^2} , \tag{2.12}$$

showing that the contribution of the wiggling term to α_1 is very appreciable.

III. COMPUTATION OF MOMENTUM COMPACTION FACTOR

1. Differential equation for momentum dispersion

To compute the momentum compaction to first order in δ, we require the differential equation for the momentum dispersion function η also to first order in δ. This equation is complicated. For the FODO-cell lattice with thin quadrupoles, it reads

$$\eta'' = \frac{1}{\rho_0} \left\{ \left(1 - \frac{\eta}{\rho_0} \right) - \delta \left[\left(1 - \frac{\eta}{\rho_0} \right)^2 - \frac{\eta'^2}{2} \right] \right\} - (1 - \delta) \eta K , \tag{3.1}$$

where the prime is differentiation with respect to the distance along the designed orbit, and

$$K = \left. \frac{B'}{B_0 \rho_0} \right|_{x=0} + \left. \frac{B''}{2 B_0 \rho_0} \right|_{x=0} \eta \delta + \cdots \tag{3.2}$$

depicts the quadrupole field, sextupole field, etc., with B_0 representing the dipole bending field. Here, B'/B_0 is positive (negative) for an F-quadrupole (D-quadrupole). In Eq. (3.1), $\mathcal{O}(\delta^2)$ has been neglected. This equation as well as the one accurate to all orders of δ are derived in Appendix A. The solution of Eq. (3.1) in this simplified FODO cell and the eventual integrations of Eq. (2.9) for each order of δ are straightforward but extremely tedious, if we wish to keep all orders of of the bending angle θ_0 of the half-cell dipole. The latter is important when the accelerator ring is small. The tedious part is the solution through the dipole. In fact, the trajectory through the dipole is just the arc of a simple circle of known radius. It becomes difficult

in Eq. (3.1) because the coordinate system moves along the accelerator ring, or the coordinates are curvilinear.[7] For this reason, we discard the differential equation and resort to a geometric method instead, where no solution of differential equation or integration will be necessary. After we obtain the solution, we will check in Appendix B that Eq. (3.1) is indeed correct.

2. The geometric approach

Consider a half cell shown in Fig. 2. The half F-quadrupole is at FF' while the half D-quadrupole is at DD'. In between lies the dipole of bend angle θ_0. The designed orbit in the half cell is the arc FD and is of length $\ell_0 = \rho_0\theta_0$ with radius of curvature ρ_0, while the off-momentum closed orbit corresponding to δ is the arc $F'D'$ and is of length ℓ, radius of curvature ρ, and bend angle $\theta = \ell/\rho$. Passing through the thin half F-quadrupole, the off-momentum orbit acquires, according to the bending due to the Lorentz force, an angular change of

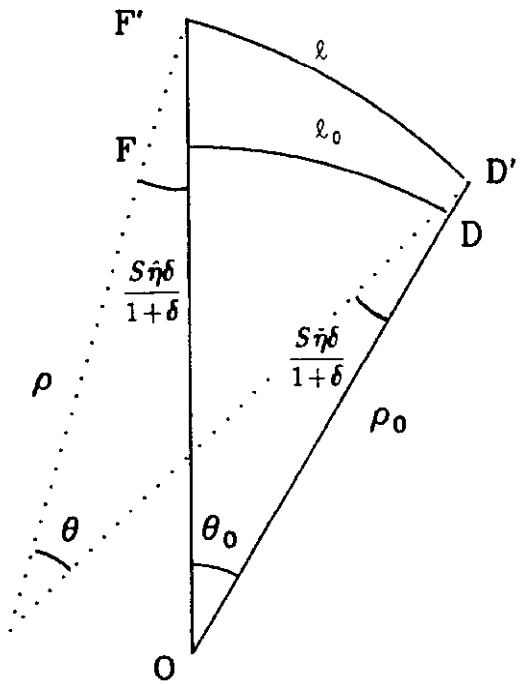

Figure 2: Solution of momentum compaction factor in flat (non-curvilinear) coordinates.

$$\Delta\phi_F = \frac{p_0}{p}\int ds \frac{B'\hat{\eta}\delta}{B_0\rho_0} = \frac{S\hat{\eta}}{\ell_0}\frac{\delta}{1+\delta} , \tag{3.3}$$

where Eq. (2.11) has been used. The off-momentum orbit then turns through an angle θ inside the dipole and another

$$\Delta\phi_D = -\frac{S\check{\eta}}{\ell_0}\frac{\delta}{1+\delta} , \tag{3.4}$$

through the half D-quadrupole to complete the half cell. In the above, the accents $\hat{}$ and $\check{}$ have been used to represent, respectively, values at the F- and D-quadrupoles. The total angle turned is obviously θ_0. Therefore,

$$\theta = \theta_0 - \frac{S\delta}{1+\delta}\frac{\hat{\eta}-\check{\eta}}{\ell_0} . \tag{3.5}$$

Since the two orbits are in the same dipole field, their radii of curvature are related by

$$\rho = \rho_0(1+\delta) . \tag{3.6}$$

Combining Eqs. (3.4) to (3.6), we have for the two orbit lengths exactly

$$\ell = \ell_0\left[1+\delta\left(1-\frac{S}{\theta_0}\frac{\hat{\eta}-\check{\eta}}{\ell_0}\right)\right] . \tag{3.7}$$

With the expansions

$$\begin{aligned}\hat{\eta} &= \hat{\eta}_0 + \hat{\eta}_1\delta + \mathcal{O}(\delta^2) ,\\ \check{\eta} &= \check{\eta}_0 + \check{\eta}_1\delta + \mathcal{O}(\delta^2) ,\end{aligned} \tag{3.8}$$

and comparison with Eq. (1.1), we arrive at

$$\begin{aligned}\alpha_0 &= 1 - \frac{S}{\theta_0}\frac{\hat{\eta}_0-\check{\eta}_0}{\ell_0} ,\\ \alpha_0\alpha_1 &= -\frac{S}{\theta_0}\frac{\hat{\eta}_1-\check{\eta}_1}{\ell_0} ,\end{aligned} \tag{3.9}$$

which are exact to all orders of θ_0. We shall demonstrate in Appendix C that the differential equation (3.1) for the momentum dispersion function also leads to these same expressions for α_0 and $\alpha_0\alpha_1$.

3. Solution of dispersions at F- and D-quadrupoles

The off-momentum closed orbit $F'D'$ is an arc of a circle with radius $\rho = \rho_0(1+\delta)$. The equation of the arc contains only two constants plus $\hat{\eta}$ and $\check{\eta}$. However, this arc is constrained by its positions and slopes at the dipole's entrance and exit. Therefore the two constants together with $\hat{\eta}$ and $\check{\eta}$ can be determined.

Consider OF' of Fig. 2 as the y-axis and O the origin. The x-axis is on the dipole side of OF'. The point F' is $(0, \rho_0+\hat{\eta}\delta)$ and the arc $F'D'$ is at an angle $S\hat{\eta}\delta/(1+\delta)$. The equation of the arc $F'D'$ is therefore given by

$$\left[x + \rho \sin \frac{S\hat{\eta}\delta}{1+\delta}\right]^2 + \left[y - \rho_0 - \hat{\eta}\delta + \rho \cos \frac{S\hat{\eta}\delta}{1+\delta}\right]^2 = \rho^2 \ . \tag{3.10}$$

In the above, ℓ_0 has been removed since we have simplified the notations by measuring all lengths in terms of it. Now rotate the x- and y-axes by an angle $\theta_0/2$ so that the new y-axis passes through the center of the dipole. In terms of the new axes, the equation of the circular arc becomes

$$\left[x \cos \frac{\theta_0}{2} + y \sin \frac{\theta_0}{2} + \rho \sin \frac{S\hat{\eta}\delta}{1+\delta}\right]^2 + \left[-x \sin \frac{\theta_0}{2} + y \sin \frac{\theta_0}{2} - \rho_0 - \hat{\eta}\delta + \rho \cos \frac{S\hat{\eta}\delta}{1+\delta}\right]^2 = \rho^2 \ . \tag{3.11}$$

We can also start with OD' as the y-axis. The angle at D' is now $S\check{\eta}\delta/(1+\delta)$. The axes are then rotated in the opposite direction by $\theta_0/2$ so that the equation of the arc $F'D'$ becomes

$$\left[x \cos \frac{\theta_0}{2} - y \sin \frac{\theta_0}{2} + \rho \sin \frac{S\check{\eta}\delta}{1+\delta}\right]^2 + \left[x \sin \frac{\theta_0}{2} + y \sin \frac{\theta_0}{2} - \rho_0 - \check{\eta}\delta + \rho \cos \frac{S\check{\eta}\delta}{1+\delta}\right]^2 = \rho^2 \ . \tag{3.12}$$

Equations (3.10) and (3.11) are exactly the same because they describe the same arc $F'D'$. By equating coefficients, we obtain

$$\rho \sin \frac{S\hat{\eta}\delta}{1+\delta} - \left[\rho \cos \frac{S\hat{\eta}\delta}{1+\delta} - \hat{\eta}\delta\right] t = \rho \sin \frac{S\check{\eta}\delta}{1+\delta} + \left[\rho \cos \frac{S\check{\eta}\delta}{1+\delta} - \check{\eta}\delta\right] t \ , \tag{3.13}$$

$$t\rho \sin \frac{S\hat{\eta}\delta}{1+\delta} + \left[\rho \cos \frac{S\hat{\eta}\delta}{1+\delta} - \hat{\eta}\delta\right] = -t\rho \sin \frac{S\check{\eta}\delta}{1+\delta} + \left[\rho \cos \frac{S\check{\eta}\delta}{1+\delta} - \check{\eta}\delta\right] , \tag{3.14}$$

$$\rho^2 \sin^2 \frac{S\hat{\eta}\delta}{1+\delta} + \left[\rho \cos \frac{S\hat{\eta}\delta}{1+\delta} - \rho_0 - \check{\eta}\delta\right]^2 = \rho^2 \sin^2 \frac{S\check{\eta}\delta}{1+\delta} + \left[\rho \cos \frac{S\check{\eta}\delta}{1+\delta} - \rho_0 - \check{\eta}\delta\right]^2 , \tag{3.15}$$

where the notation $t = \tan\theta_0/2$ has been used. Any two of the above equations will give us the exact solution of $\hat{\eta}$ and $\check{\eta}$ to all orders of θ_0 and δ. Since we are interested in solution up to the first order in δ only, Eqs. (3.13) and (3.14) can be expanded and simplified to obtain for the zeroth order in δ,

$$\begin{pmatrix} 1 & -t \\ t & 1 \end{pmatrix} \begin{pmatrix} S\hat{\eta}_0 \\ 1 - \theta_0\hat{\eta}_0 \end{pmatrix} = \begin{pmatrix} 1 & t \\ -t & 1 \end{pmatrix} \begin{pmatrix} S\check{\eta}_0 \\ 1 - \theta_0\check{\eta}_0 \end{pmatrix} , \tag{3.16}$$

and for the first order in δ,

$$\begin{pmatrix} 1 & -t \\ t & 1 \end{pmatrix} \begin{pmatrix} S\hat{\eta}_1 \\ -\theta_0\hat{\eta}_1 - \frac{1}{2}S^2\hat{\eta}_0^2 \end{pmatrix} = \begin{pmatrix} 1 & t \\ -t & 1 \end{pmatrix} \begin{pmatrix} S\check{\eta}_1 \\ -\theta_0\check{\eta}_1 - \frac{1}{2}S^2\check{\eta}_0^2 \end{pmatrix} . \tag{3.17}$$

Solutions can now be obtained easily. For the zeroth order, one readily gets

$$\begin{cases} \hat{\eta}_0 - \check{\eta}_0 &= \dfrac{2St}{S^2 + \theta_0^2} \\ \hat{\eta}_0 + \check{\eta}_0 &- \dfrac{2\theta_0}{S^2 + \theta_0^2} , \end{cases} \tag{3.18}$$

or

$$\hat{\eta}_0,\ \check{\eta}_0 = \frac{\theta_0 \pm St}{S^2 + \theta_0^2} . \tag{3.19}$$

For the first order, we have

$$\begin{cases} \hat{\eta}_1 - \check{\eta}_1 &= -\dfrac{S^3 t(S^2t^2 + 3\theta_0^2)}{(S^2 + \theta_0^2)^3} \\ \hat{\eta}_1 + \check{\eta}_1 &= -\dfrac{S^2(S^2\theta_0 t^2 - 2S^2\theta_0 + \theta_0^3)}{(S^2 + \theta_0^2)^3} . \end{cases} \tag{3.20}$$

4. α_0 and α_1

Substituting Eqs. (3.18) and (3.20) into Eq. (3.9), we arrive at

$$\alpha_0 = 1 - \frac{2S^2t}{\theta_0(S^2 + \theta_0^2)} , \tag{3.21}$$

and

$$\alpha_1 = \frac{S^4 t(S^2 t^2 + 3\theta_0^2)}{(S^2+\theta_0^2)^2[\theta_0(S^2+\theta_0^2) - 2S^2 t]} \ . \tag{3.22}$$

In the situation of a very large ring where $\theta_0 \ll S$, the above expressions reduce to

$$\alpha_0 \to \frac{\theta_0(1 - S^2/12)}{S^2} \ , \tag{3.23}$$

$$\alpha_1 \to \frac{3}{2}\left(\frac{1+S^2/12}{1-S^2/12}\right) \ . \tag{3.24}$$

The value of α_1 is plotted as a function of S in Fig. 3 for simplified FODO rings consisting of $N = \pi/\theta_0$ cells. We see that higher orders in θ_0 are indeed important for rings with a small number of cells.

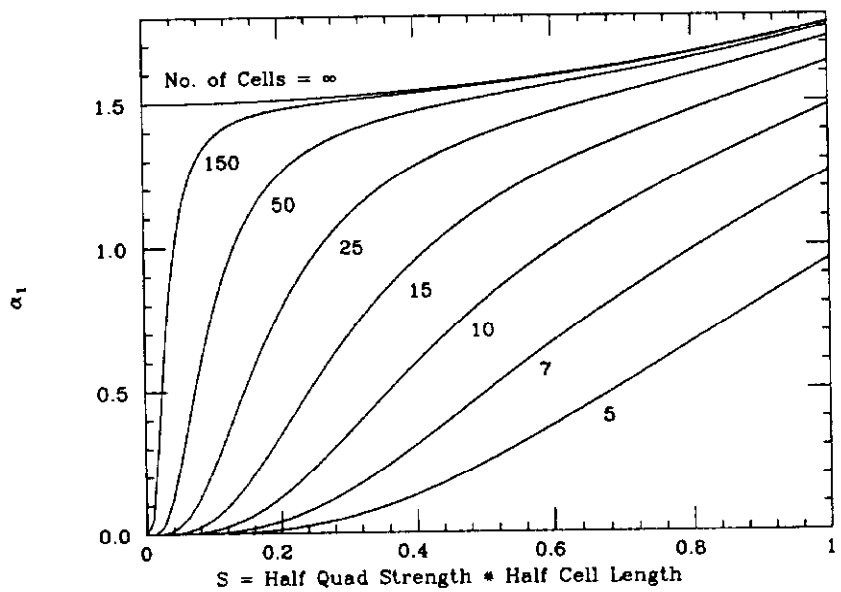

Figure 3: Plot of α_1 vs quadrupole strength for the simplified FODO lattice with different number of cells.

IV. COMPARISON WITH RESULTS FROM SYNCH

A lattice was setup as input to SYNCH containing $N = 150$ equal FODO cells. The half cell starts with a half F-quadrupole of length 5×10^{-8} m which is considered

negligible, a sector dipole of *arc* length $\ell_0 = 2\pi$ m, and a half D-quadrupole of the same length but opposite strength as the F-quadrupole. A value of S was read and the quadrupole strength was computed as S/ℓ_0. The nominal momentum used was 120 GeV/c.

At an offset momentum p, the transition gamma γ_t is defined as

$$\gamma_t^{-2} = \frac{p}{C}\frac{dC}{dp} \ . \tag{4.1}$$

With the aid of Eq. (1.1), it is easy to get

$$\gamma_t(p) = \gamma_{t0}\left[1 - \left(\alpha_1 + \frac{1}{2} - \frac{\alpha_0}{2}\right)\delta + \mathcal{O}(\delta^2)\right] \ , \tag{4.2}$$

where γ_{t0} is the transition gamma at nominal momentum p_0. Thus,

$$\alpha_1 = -\frac{1}{\gamma_{t0}}\frac{d\gamma_t}{d\delta} - \frac{1}{2} + \frac{\alpha_0}{2} \ . \tag{4.3}$$

The closed orbits for momentum offsets from $\delta = -0.0001$ to $+0.0001$ in steps of 0.0001 were computed by SYNCH and the transition gamma γ_t in each case was recorded. Momentum offsets of such small values were carefully chosen in order to ensure the stability of the lattice, especially when S or the focussing power of the quadrupoles is small. The derivative $d\gamma_t/d\delta$ was obtained by using a 3-point centered formula. The quadrupole strength S was varied from 0.01 to 0.99. The α_1 obtained is plotted in Fig. 4 together with the theoretical curve given by Eq. (3.22). From the plot, no deviations can be observed visually. If we look into the actual numerical values listed in Table I, we see that the agreement has been good up to 3 significant figures, except in the region where S is small. The typical value of γ_t is 24 when $S \sim 0.5$ and the SYNCH results provide 5 figures after the decimal point. However, the biggest variation for $\delta = \pm 0.0001$ is the last 3 figures after the decimal and much less when s is small.

A similar test was performed with a lattice consisting of only $N = 15$ FODO cells and all other parameter unchanged. Here, the lattice is less stable at big momentum offset. We again offset the momentum by $\delta = \pm 0.0001$ and employed a 3-point centered formula to evaluate the derivative of γ_t. The results are plotted in Fig. 5 and listed in Table II. The differences between the SYNCH values and theory are

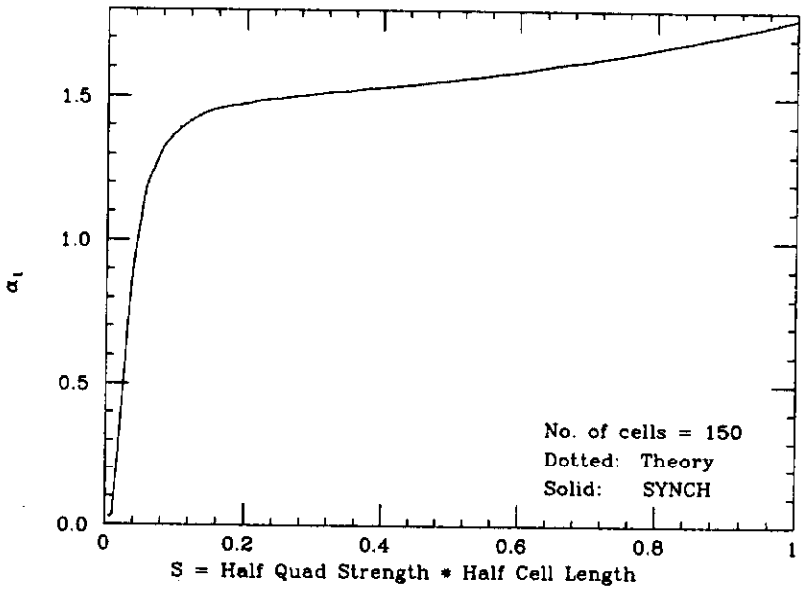

Figure 4: Comparison of SYNCH computation of α_1 with theory for the simplified FODO lattice consisting of $N = 150$ identical cells.

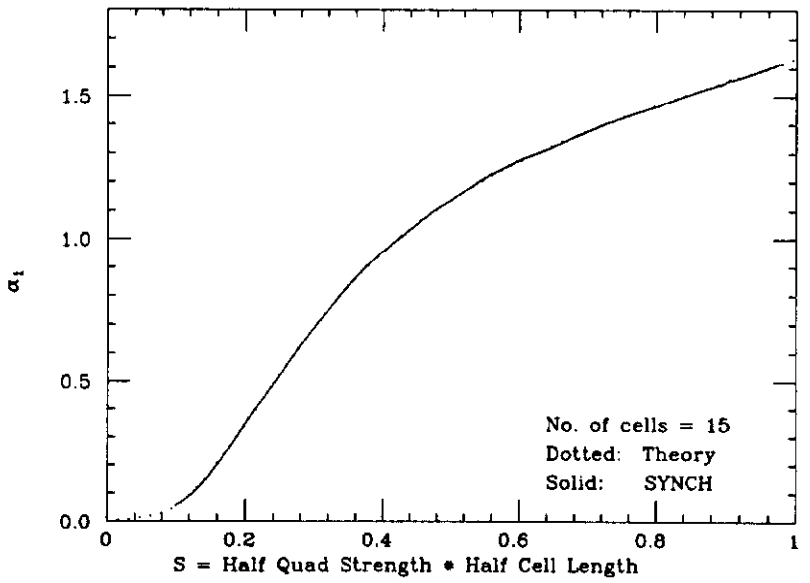

Figure 5: Comparison of SYNCH computation of α_1 with theory for the simplified FODO lattice consisting of only $N = 15$ identical cells.

S	γ_{t0}	α_1		
		SYNCH	Theory	Difference
0.020	1.38273	0.340	0.341	−0.001
0.040	2.15596	0.930	0.924	0.005
0.060	3.03476	1.202	1.193	0.009
0.080	3.94950	1.317	1.315	0.002
0.100	4.88028	1.375	1.379	−0.004
0.120	5.81968	1.413	1.416	−0.003
0.140	6.76442	1.440	1.440	0.000
0.175	8.42602	1.465	1.465	0.000
0.200	9.61756	1.476	1.478	−0.002
0.250	12.00975	1.493	1.495	−0.001
0.300	14.41296	1.507	1.508	−0.001
0.350	16.82727	1.519	1.520	−0.001
0.400	19.25354	1.532	1.532	0.000
0.450	21.69299	1.543	1.545	−0.002
0.500	24.14703	1.557	1.558	−0.001
0.550	26.61723	1.573	1.573	0.000
0.600	29.10524	1.588	1.589	−0.001
0.650	31.61283	1.607	1.606	0.001
0.700	34.14183	1.624	1.625	−0.001
0.750	36.69417	1.646	1.645	0.001
0.800	39.27188	1.667	1.667	0.001
0.850	41.87708	1.690	1.690	0.000
0.900	44.51200	1.715	1.715	0.000
0.950	47.17899	1.742	1.742	0.000
0.995	49.60875	1.768	1.768	0.000
0.999	49.82614	1.771	1.771	0.000

Table I: Comparison of SYNCH with theory for the simplified lattice consisting of 150 FODO cells and thin quadrupoles.

S	γ_{t0}	α_1		
		SYNCH	Theory	Difference
0.020	1.38273	0.340	0.341	−0.001
0.040	2.15596	0.933	0.924	0.009
0.060	3.03476	1.205	1.193	0.012
0.080	3.94950	1.317	1.315	0.002
0.100	4.88028	1.375	1.379	−0.004
0.120	5.81968	1.412	1.416	−0.004
0.140	6.76442	1.440	1.440	0.000
0.175	8.42602	1.465	1.465	0.000
0.200	9.61756	1.475	1.478	−0.003
0.250	12.00975	1.493	1.495	−0.002
0.300	14.41296	1.508	1.508	0.000
0.350	16.82727	1.519	1.520	−0.001
0.400	19.25354	1.532	1.532	0.000
0.450	21.69299	1.543	1.545	−0.002
0.500	24.14703	1.557	1.558	−0.002
0.550	26.61723	1.572	1.573	−0.001
0.600	29.10524	1.587	1.589	−0.002
0.650	31.61283	1.608	1.606	0.001
0.700	34.14183	1.624	1.625	−0.001
0.750	36.69417	1.645	1.645	0.000
0.800	39.27188	1.667	1.667	0.001
0.850	41.87708	1.690	1.690	0.000
0.900	44.51200	1.715	1.715	0.000
0.950	47.17899	1.742	1.742	−0.001
0.995	49.60875	1.768	1.768	0.000
0.999	49.82614	1.771	1.771	0.001

Table II: Comparison of SYNCH with theory for the simplified lattice consisting of 15 FODO cells and thin quadrupoles.

bigger here due to the lesser stability of the lattice and the lesser accuracy in the evaluation of the derivatives. However, the agreement is still excellent.

In all cases, the values of the on-momentum γ_t provided by SYNCH agree with the theoretical values given by Eq. (3.21) up to all the five figures after the decimal point.

V. CHROMATICITY CORRECTIONS

The natural chromaticities in this lattice can be corrected by placing half "thin" sextupoles of strength

$$S_F = \int d\ell \frac{B''_{S_F}}{2B_0\rho_0} \tag{5.1}$$

on each side of the "thin" F-quadrupole and half "thin" sextupoles of strength

$$S_D = \int d\ell \frac{B''_{S_D}}{2B_0\rho_0} \tag{5.2}$$

on each side of the "thin" D-quadrupole. The angle the off-momentum orbit turns at the half F-quadrupole and half F-sextupole changes from Eq. (3.3) to

$$\Delta\phi_F = \frac{S\hat{\eta}\delta}{1+\delta} + \frac{S_F\hat{\eta}^2\delta^2}{1+\delta} \ . \tag{5.3}$$

Similarly, at the half D-sextupole and half D-quadrupole the angle turned changes from Eq. (3.4) to

$$\Delta\phi_D = -\frac{S\check{\eta}\delta}{1+\delta} + \frac{S_D\check{\eta}^2\delta^2}{1+\delta} \ . \tag{5.4}$$

This implies no change in all the zeroth-order (in δ) equations and expressions. To obtain the first-order equations and expressions, however, we have to make the substitutions:

$$\begin{cases} S\hat{\eta}_1 \ \rightarrow \ S\hat{\eta}_1 + S_F\hat{\eta}_0^2 \ , \\ S\check{\eta}_1 \ \rightarrow \ S\check{\eta}_1 - S_D\check{\eta}_0^2 \ . \end{cases} \tag{5.5}$$

We therefore have, instead of Eq. (3.9),

$$\alpha_0\alpha_1 = -\frac{1}{\theta_0}\left[S(\hat{\eta}_1 - \check{\eta}_1) + (S_F\hat{\eta}_0^2 + S_D\check{\eta}_0^2)\right] \ . \tag{5.6}$$

Instead of Eq. (3.17), we have

$$\begin{pmatrix} 1 & -t \\ t & 1 \end{pmatrix} \begin{pmatrix} S\hat{\eta}_1 + S_F\hat{\eta}_0^2 \\ -\theta_0\hat{\eta}_1 - \frac{1}{2}S^2\hat{\eta}_0^2 \end{pmatrix} = \begin{pmatrix} 1 & t \\ -t & 1 \end{pmatrix} \begin{pmatrix} S\check{\eta}_1 - S_D\check{\eta}_0^2 \\ -\theta_0\check{\eta}_1 - \frac{1}{2}S^2\check{\eta}_0^2 \end{pmatrix} . \tag{5.7}$$

Solving Eq. (5.7) for $\hat{\eta}_1 - \check{\eta}_1$ and substituting in Eq. (5.6), we arrive at

$$\alpha_0\alpha_1 = \frac{S^4t(S^2t^2+3\theta_0^2)}{\theta_0(S^2+\theta_0^2)^3} - (S_F\hat{\eta}_0^3 + S_D\check{\eta}_0^3) . \tag{5.8}$$

The last term is the contribution due to the sextupoles.

If one desires to cancel a fraction f of the horizontal and vertical natural chromaticities, the sextupole strengths need to be chosen as

$$2S_F\hat{\eta}_0 = fS \qquad \text{and} \qquad -2S_D\check{\eta}_0 = fS , \tag{5.9}$$

which turns Eq. (5.8) into

$$\alpha_0\alpha_1 = \frac{S^4t(S^2t^2+3\theta_0^2)}{\theta_0(S^2+\theta_0^2)^3} - \frac{2fS^2\theta_0t}{(S^2+\theta_0^2)^2} . \tag{5.10}$$

In the limit of $\theta_0 \ll S$, α_1 in Eq. (3.24) becomes

$$\alpha_1 \to \frac{\frac{3}{2}\left(1+\frac{S^2}{12}\right) - f}{1-\frac{S^2}{12}} . \tag{5.11}$$

We see that $\alpha_1 \approx 3/2$ without chromaticity correction ($f = 0$), and reduces to $\approx 1/2$ with complete correction ($f = 1$).

VI. CONCLUSION

We have derived the differential equation for the momentum dispersion function accurate for all orders of momentum offset and all orders of dipole bending angle. However, to avoid solving the differential equation and doing subsequent integrations, a geometric method was used to compute α_0 and α_1 up to all orders of dipole bending angle. The lattice used consisted of only FODO cells with thin quadrupoles.

The lattice code SYNCH was used to check the theoretical derivations. We found that α_0 and α_1 for such a lattice with $N = 150$ cells and one with $N = 15$ cells agree with theory extremely well. This leads us to conclude that the SYNCH computation of momentum compaction at off-momentum is very accurate.

APPENDIX A

In this appendix, the differential equation satisfied by the momentum dispersion function η up to all orders of δ and all orders of dipole bend angle θ_0 is derived.

Consider an infinitesimal increment along the designed orbit and the same along off-momentum closed orbit in Fig. 1. Let ϕ_0 be the angle between the designed orbit at A and some reference, and ϕ be the angle between the off-momentum closed orbit at B and the same reference. The transverse offset x is denoted by AB. The rate of change in x along the designed orbit, defined by

$$x' \equiv \frac{dx}{ds} \ , \tag{A.1}$$

should be computed with care. Here, ds is the infinitesimal advance along the designed orbit and should not be confused with the S denoting the quadrupole strength in Eq. (2.11). With the help of Eq. (2.1), we have

$$x' = \frac{d\ell_0}{ds}\frac{dx}{d\ell_0} = \left(1 + \frac{x}{\rho_0}\right)\tan(\phi - \phi_0) \ , \tag{A.2}$$

where ρ_0 is the radius of curvature of the designed orbit at A. Note that Eq. (A.2) reduces to Eq. (2.2) after higher orders of δ are removed. Another order of the derivative gives

$$x'' = \frac{x'^2}{\rho_0\,(1 + x/\rho_0)} + \left(1 + \frac{x}{\rho_0}\right)\left[1 + \frac{x'^2}{(1 + x/\rho_0)^2}\right](\phi' - \phi_0') \ . \tag{A.3}$$

The change in angle of the designed orbit at A is given by

$$\phi_0' = -\frac{1}{\rho_0} \ . \tag{A.4}$$

The negative sign comes about because ϕ_0 decreases as we advance along the designed orbit. The change in the angle of the off-momentum orbit at B for the length element $d\ell$ is

$$d\phi = -\frac{eBd\ell}{p} \ . \tag{A.5}$$

Here, the magnetic field B can be expanded as

$$B = B_0 + B'|_0\, x + \left.\frac{B''}{2}\right|_0 x^2 + \cdots = B_0\rho_0\left[\frac{1}{\rho_0} + Kx\right] \ , \tag{A.6}$$

where the first term in the squared brackets is the dipole term and K in the second term, given by Eq. (3.2), includes all higher-multipoles. Combining Eqs. (A.5) and (A.6), we get

$$\phi' = -\sec(\phi - \phi_0)\frac{p_0}{p}\left(1 + \frac{x}{\rho_0}\right)\left(\frac{1}{\rho_0} + Kx\right) , \tag{A.7}$$

which certainly reduces to Eq. (A.4) when $\delta \to 0$.

Substituting Eqs. (A.4) and (A.7) in Eq. (A.6) and eliminating $\phi - \phi_0$ by Eq. (A.2), we obtain the differential equation satisfied by x; namely,

$$\begin{aligned} x'' = {} & \frac{x'^2}{\rho_0(1 + x/\rho_0)} + \left(1 + \frac{x}{\rho_0}\right)\left[1 + \frac{x'^2}{(1 + x/\rho_0)^2}\right] \times \\ & \times \left\{\frac{1}{\rho_0} - \frac{1}{1+\delta}\left[1 + \frac{x'^2}{(1 + x/\rho_0)^2}\right]^{\frac{1}{2}}\left(1 + \frac{x}{\rho_0}\right)\left(\frac{1}{\rho_0} + Kx\right)\right\} . \end{aligned} \tag{A.8}$$

The equation for the momentum dispersion is therefore

$$\begin{aligned} \eta'' = {} & \frac{\eta'^2\delta}{\rho_0(1 + \eta\delta\rho_0)} + \left(1 + \frac{\eta\delta}{\rho_0}\right)\left[1 + \frac{(\eta'\delta)^2}{(1 + \eta\delta/\rho_0)^2}\right] \times \\ & \times \left\{\frac{1}{\delta\rho_0} - \frac{1}{1+\delta}\left[1 + \frac{(\eta'\delta)^2}{(1 + \eta\delta/\rho_0)^2}\right]^{\frac{1}{2}}\left(1 + \frac{\eta\delta}{\rho_0}\right)\left(\frac{1}{\delta\rho_0} + K\eta\right)\right\} . \end{aligned} \tag{A.9}$$

Although Eqs. (A.8) and (A.9) are exact, their solutions are impossibly difficult. In this paper, we wish to solve η only up to first order in δ. Equation (A.9) can be easily expanded to give Eq. (3.1). There, the term involving K/ρ_0 has been deleted, because it vanishes for a lattice containing "thin" multipoles. Also the appearance of the η'^2 term reminds us of the wiggling contribution.

When η is expanded according to Eq. (2.6), Eq. (3.1) leads to the following equations for η_0 and η_1:

$$\eta_0'' + \eta_0\left(\frac{1}{\rho_0} + K\right) = \frac{1}{\rho_0} , \tag{A.10}$$

and

$$\eta_1'' + \eta_1\left(\frac{1}{\rho_0} + K\right) = -\frac{1}{\rho_0}\left[\left(1 + \frac{\eta_0}{\rho_0}\right)^2 - \frac{\eta_0'^2}{2\rho_0}\right] + \eta_0 K , \tag{A.11}$$

which can be solved straightforwardly.

APPENDIX B

The momentum dispersion function η at any point inside the dipole can also be solved easily using the geometric approach. Consider Eq. (3.10) and rotate the axes clockwise by any angle θ. The new equation is exactly Eq. (3.11) with $\theta_0/2$ replaced by θ. Now let

$$\begin{cases} x &= 0 \\ y &= \rho_0 + \eta(\theta)\delta \ , \end{cases} \tag{B.1}$$

and expand the equation up to second order in δ. The dispersion function can then be solved:

$$\eta_0(\theta) = \left(\cos\theta - \frac{S}{\theta_0}\sin\theta\right)\hat{\eta}_0 - \frac{\cos\theta - 1}{\theta_0} \ , \tag{B.2}$$

$$\eta_1(\theta) = \left(\cos\theta - \frac{S}{\theta_0}\sin\theta\right)\hat{\eta}_1 + \frac{S^2}{2\theta_0}\cos(\theta)\hat{\eta}_0^2 - \frac{\eta_0'^2}{2\theta_0} \ , \tag{B.3}$$

where again we measure every length in units of the half-cell length ℓ_0 so that $1/\rho_0$ is replaced by θ_0. In the above, η_0' is the derivative with respect to advance along the designed orbit; or $\eta_0' = \theta_0 d\eta_0/d\theta$. We have verified that these expressions satisfy the differential equations (A.10) and (A.11). Also they give the correct values at the dipole's exit as the previously computed results of Eqs. (3.19) and (3.20). Their slopes at both the dipole's entrance and exit also give the correct values as predicted. Integration of η_0 in Eq. (B.2) gives α_0 as expressed by Eq. (3.21). We can rearrange Eq. (B.3) and integrate to get

$$\int_0^{\theta_0} d\theta \left(\eta_1 + \frac{\eta_0'^2}{2\theta_0}\right) = \frac{S^4 t(S^2t^2 + 3\theta_0^2)}{\theta_0(S^2 + \theta_0)^3} \ , \tag{B.4}$$

which is just $\alpha_0\alpha_1$ given by Eqs. (3.21) and (3.22).

APPENDIX C

In this section, we try to make use of the differential equations (A.10) and (A.11) to derive the expression for α_0 and α_1 as given by Eq. (3.9).

From Eqs. (A.2), (3.3), and (3.4), we can write down the expressions for x' at the entrance and exit of the dipole:

$$\begin{cases} \hat{x}' &= -S\hat{\eta}\delta[1 - \delta(1 - \hat{\eta}\theta_0) + \mathcal{O}(\delta^2)] \\ \check{x}' &= -S\check{\eta}\delta[1 - \delta(1 - \check{\eta}\theta_0) + \mathcal{O}(\delta^2)] \ , \end{cases} \tag{C.1}$$

For the derivative of the dispersion function, we have

$$\begin{cases} \hat{\eta}_0' + \hat{\eta}_1'\delta &= -S[\hat{\eta}_0 + \delta(\hat{\eta}_1 - \hat{\eta}_0 + \hat{\eta}_0^2\theta_0)] \\ \check{\eta}_0' + \check{\eta}_1'\delta &= -S[\check{\eta}_0 + \delta(\check{\eta}_1 - \check{\eta}_0 + \check{\eta}_0^2\theta_0)] \ . \end{cases} \tag{C.2}$$

We now integrate Eq. (A.10) from the dipole's entrance to the dipole's exit. We get

$$\int_{\ell_0} ds\, \theta_0(1 - \eta_0\theta_0) = -S(\hat{\eta}_0 - \check{\eta}_0) \ , \tag{C.3}$$

which gives the expression of α_0 as given by Eq. (3.9) immediately when expression (2.8) is employed.

We next integrate Eq. (A.11) and rewrite it in the form

$$\alpha_0\alpha_1 = \int_{\ell_0} ds \left(\eta_1\theta_0 + \frac{1}{2}\,\eta_0'^2\right) = \int_{\ell_0} ds \left[(\eta_0\theta_0 - 1) + \left(\eta_0\theta_0 - \eta_0\theta_0^2 + \eta_0'^2\right)\right] + \theta_0\Delta\eta_1' \ , \tag{C.4}$$

where as given by Eq. (C.2),

$$\Delta\eta_1' = -S\left[(\hat{\eta}_1 - \check{\eta}_1) - (\hat{\eta}_0 - \check{\eta}_0) + \theta_0(\hat{\eta}_0^2 - \check{\eta}_0^2)\right] \ . \tag{C.5}$$

The first term in the squared brackets of Eq. (C.4) is just α_0 which cancels the $\hat{\eta}_0 - \check{\eta}_0$ term in Eq. (C.5). For the last term in the squared brackets of Eq. (C.4), we integrate $\eta_0'^2$ by parts and make use of Eq. (A.10) to eliminate η''. The whole integral for this last term then vanishes leaving behind the integrated part

$$\Delta\eta\eta' = \check{\eta}_0\check{\eta}_0' - \hat{\eta}_0\hat{\eta}_0' = S(\hat{\eta}_0^2 - \check{\eta}_0^2) \ , \tag{C.6}$$

which cancels the last term in $\Delta\eta_1'$. It is then easy to conclude that Eq. (C.4) indeed reproduces Eq. (3.9).

REFERENCES

1. K. Johnsen, *Effects of Nonlinearities on Phase Transition,* Proc. of CERN Symposium on High Energy Accelerators and Pion Physics, Geneva, 1956, Vol. 1, p. 106. Note that there are many different notations and definitions for the expansion of the momentum compaction. For example, our α_0 and α_1 are named α_1 and α_2 in this reference.

2. C. Pellegrini and D. Robin, *Quasi-isochronous Storage Ring,* Nucl. Inst. Meth. **A301**, 27 (1991).

3. S. Peggs, *Transition Crossing Time Shifts,* Fermilab Internal Report AP Note90-004, 1990.

4. A.A. Garren, A.S. Kenney, E.D. Courant, and M.J. Syphers, *A User's Guide to SYNCH,* Fermilab Internal Report FN-420, 1985.

5. A. Bogacz, private communication. A. Bogacz and S. Peggs, *Comments on the Behavior of* α_1 *in Main Injector* γ_t*-jump Schemes,* Proc. of the Fermilab III Instabilities Workshop, Fermilab, Batavia, 1990, p. 192.

6. see for example, E. Ciapala, A. Hoffman, S. Myers, and T. Risselada, *The Variation of* γ_t *with* $\Delta p/p$ *in the CERN ISR,* IEEE **N3**, 3571 (1979); R. Cappi, J.P. Delahaye, and K.H. Reich, *PS Beam Measurements at Flat-top Fields near Transition Energy*, IEEE **N23**, 2389 (1981).

7. J. Shan, *et al, The Condition for Isochronism in Synchrotrons and Storage Rings,* Fermilab Internal Report, to be published. In this reference, the authors try to solve the differential equation for the momentum dispersion function directly up to first order in δ and compute α_0 and α_1 by performing the integrations (2.8) and (2.9).